HHS Public Access

Author manuscript

Mol Cell Neurosci. Author manuscript; available in PMC 2025 September 01.

Published in final edited form as:

Mol Cell Neurosci. 2024 September ; 130: 103954. doi:10.1016/j.mcn.2024.103954.

iPSC-induced neurons with the V337M *MAPT* mutation are selectively vulnerable to caspase-mediated cleavage of tau and apoptotic cell death

Panos Theofilas[1], **Chao Wang**[2], **David Butler**[3], **Dulce O. Morales**[1], **Cathrine Petersen**[1], **Andrew Ambrose**[10], **Brian Chin**[4], **Teddy Yang**[4], **Shireen Khan**[5], **Raymond Ng**[5], **Rakez Kayed**[6], **Celeste M. Karch**[7], **Bruce L. Miller**[1], **Jason E. Gestwicki**[8], **Li Gan**[2,9], **Sally Temple**[3], **Michelle R. Arkin**[10,*], **Lea T. Grinberg**[1,11,*]

[(1)]Memory and Aging Center, Department of Neurology, UCSF, San Francisco, CA, USA

[(2)]Gladstone Institute of Neurological Disease, San Francisco, CA, USA

[(3)]Neural Stem Cell Institute, Rensselaer, NY, USA

[(4)]Shanghai ChemPartner, Shanghai, China

[(5)]ChemPartner San Francisco, South San Francisco, CA, USA

[(6)]Department of Neurology, University of Texas Medical Branch, Galveston, TX, USA

[(7)]Washington University School of Medicine, St Louis, MO, USA

[(8)]Department of Pharmaceutical Chemistry, UCSF, San Francisco, CA, USA

[(9)]Helen and Robert Appel Alzheimer's Disease Research Institute, Brain and Mind Research Institute, Weill Cornell Medicine, New York, NY, USA

[(10)]Department of Pharmaceutical Chemistry and Small Molecule Discovery Center, UCSF, San Francisco, CA, USA

[*]**Correspondence:** Lea T. Grinberg, MD, PhD; John Douglas French Alzheimer's Foundation Endowed Professor. Associate Professor of Neurology and Pathology; University of California, San Francisco; 675 Nelson Rising Lane, 211B, Box 1207; San Francisco, CA 94158; lea.grinberg@ucsf.edu; Michelle R. Arkin, PhD; Thomas William and Frederick John MacWilliam Distinguished Professor and Chair of Pharmaceutical Chemistry; School of Pharmacy, University of California San Francisco; Box 2552; 1700 4th Street. San Francisco, CA. 94143; Michelle.arkin@ucsf.edu.

[*]Co-senior authors

Authors' contributions

P.T., M.R.A., and L.T.G. designed the study; P.T. performed the experiments, data acquisition, and analyses. B.C., T.Y., S. K., R.N., A.J.A., and M.R.A. generated the neoepitope caspase-cleaved tau antibodies. R.K. provided the oligomeric tau antibody and contributed to data interpretation. C.W. and L.G. provided the iPSC lines, C.P. contributed to data analyses and graphic design, D.B., C.W., D.O.M., C.M.K, J.E.G., and S.T. contributed with cell culture work and data interpretation, B.L.M and L.T.G provided the human brain specimens, P.T. wrote the manuscript, C.W., D.B., R.N., S.T., M.R.A., and L.T.G. revised the manuscript, L.T.G. and M.R.A. supervised the study and approved the submitted version. All authors read and approved the final manuscript.

Ethics approval and consent to participate

The use of human brain tissue and iPSC-derived induced neurons from humans has been approved by the University of California San Francisco Institutional Review Board.

Availability of data and materials

The data that support the findings of this study are available from the corresponding authors upon reasonable request.

Competing interests

Michelle R. Arkin is cofounder of Elgia Therapeutics, which is developing caspase-6 inhibitors for inflammatory diseases. The other authors have declared no conflict of interest.

[11]Department of Pathology, University of Sao Paulo Medical School

Abstract

Background: Tau post-translational modifications (PTMs) result in the gradual build-up of abnormal tau and neuronal degeneration in tauopathies, encompassing variants of frontotemporal lobar degeneration (FTLD) and Alzheimer's disease (AD). Tau proteolytically cleaved by active caspases, including caspase-6, may be neurotoxic and prone to self-aggregation. Also, our recent findings show that caspase-6 truncated tau represents a frequent and understudied aspect of tau pathology in AD in addition to phospho-tau pathology. In AD and Pick's disease, a large percentage of caspase-6 associated cleaved-tau positive neurons lack phospho-tau, suggesting that many vulnerable neurons to tau pathology go undetected when using conventional phospho-tau antibodies and possibly will not respond to phospho-tau based therapies. Therefore, therapeutic strategies against caspase cleaved-tau pathology could be necessary to modulate the extent of tau abnormalities in AD and other tauopathies.

Methods: To understand the timing and progression of caspase activation, tau cleavage, and neuronal death, we created two mAbs targeting caspase-6 tau cleavage sites and probed postmortem brain tissue from an individual with FTLD due to the V337M *MAPT* mutation. We then assessed tau cleavage and apoptotic stress response in cortical neurons derived from induced pluripotent stem cells (iPSCs) carrying the FTD-related V337M *MAPT* mutation. Finally, we evaluated the neuroprotective effects of caspase inhibitors in these iPSC-derived neurons.

Results: FTLD V337M *MAPT* postmortem brain showed positivity for both cleaved tau mAbs and active caspase-6. Relative to isogenic wild-type *MAPT* controls, V337M *MAPT* neurons cultured for 3 months post-differentiation showed a time-dependent increase in pathogenic tau in the form of caspase-cleaved tau, phospho-tau, and higher levels of tau oligomers. Accumulation of toxic tau species in V337M *MAPT* neurons was correlated with increased vulnerability to pro-apoptotic stress. Notably, this mutation-associated cell death was pharmacologically rescued by the inhibition of effector caspases.

Conclusions: Our results suggest an upstream, time-dependent accumulation of caspase-6 cleaved tau in V337M *MAPT* neurons promoting neurotoxicity. These processes can be reversed by caspase inhibition. These results underscore the potential of developing caspase-6 inhibitors as therapeutic agents for FTLD and other tauopathies. Additionally, they highlight the promise of using caspase-cleaved tau as biomarkers for these conditions.

Keywords

Tau cleavage; neoepitope antibody; active caspase-6; iPSCs; FTLD; V337M *MAPT* mutation; tauopathies; postmortem

Introduction

Tau post-translational modifications (PTMs) are pivotal in the pathogenesis of neurodegenerative diseases known as tauopathies, including frontotemporal lobar degeneration (FTLD) and Alzheimer's disease (AD) (Lanata and Miller, 2016; Spillantini and Goedert, 2013). Despite the critical need for effective treatments, therapeutic

strategies targeting tauopathies remain limited. While research has extensively explored tau hyperphosphorylation (phospho-tau), other tau PTMs, including those resulting from proteolytic cleavage by active caspases, are also significant but less studied (Alonso et al., 1996; Iqbal et al., 1986). In experimental models, caspase-cleaved tau promotes tau aggregation, tau spreading, and neurotoxicity (de Calignon et al., 2010; Kim et al., 2016; Nicholls et al., 2017; Rissman et al., 2004).

Caspases (cysteine-aspartic proteases) are proteolytic enzymes with well-defined roles in cell death and inflammation. Accumulating evidence supports a key pathogenic role of the effector caspase-6 in major diseases including AD, Huntington's disease, and ischemic stroke (Albrecht et al., 2007; Girling et al., 2018; Graham et al., 2006; Theofilas et al., 2022, 2018). Caspase activity correlates with progressive tau neuropathological stages and caspase levels inversely correlate with cognitive performance in aged individuals (Ramcharitar et al., 2013). Active caspases promote axonal degeneration in several cellular and *in vivo* animal models of AD (Cusack et al., 2013; Nikolaev et al., 2009). Active caspase-6 colocalizes with NFT-positive neurons in AD patients' brains (Gamblin et al., 2003; Theofilas et al., 2022, 2018; Zhang et al., 2009; Zhao et al., 2015), We previously demonstrated a positive linear correlation between progressive AD-tau neuropathological stages and increasing levels of active caspase-6 and phospho-tau colocalization in neurons in the locus coeruleus and dorsal raphe nucleus, brain regions showing the earliest vulnerability to AD-tau pathology (Theofilas et al., 2018). Moreover, we showed that in AD, the quantity of neurons exhibiting caspase-6 associated cleaved tau is comparable to those with phospho-tau. However, there is only about a 40% overlap between these two markers (Theofilas et al., 2022), highlighting that caspase-6 truncated tau is a prevalent yet often overlooked pathological feature in AD. Therefore, therapeutic strategies against caspase cleaved-tau pathology could be necessary to modulate the extent of tau abnormalities in AD. While other caspases are likely also involved in neurodegenerative disease, caspase-6 inhibition may be sufficient to reduce neuronal damage with a significant therapeutic index, since caspase-6 knockout animals are healthy and protected from AD pathology or pro-inflammatory stimuli (Angel et al., 2020; Ladha et al., 2018).

Active caspase-6 cleaves tau after aspartic acid (Asp) at multiple sites, including the well-characterized Asp421 (D421), which is involved in tau aggregation and neurotoxicity (Gamblin et al., 2003; Klaiman et al., 2008; Rissman et al., 2004; Cotman et al., 2005; de Calignon et al., 2010; Novak et al., 1993). Caspase-6 cleaves tau at additional sites, including D13 (Horowitz et al., 2004) and D402 (Foveau et al., 2016; Guo et al., 2004; Ramcharitar et al., 2013), which are also found to mediate tau aggregation and toxicity *in vitro*. However, these cleavage sites have been less investigated compared to D421, primarily because of the limited availability of specific monoclonal antibodies (mAbs) (Horowitz et al., 2004; Guo et al., 2004).

Given the emerging importance of caspase-cleaved tau in tauopathies, this study aims to investigate the role of caspase activation, tau cleavage, and neuronal death in these conditions. We induced cortical neurons (iNs) from induced pluripotent stem cells (iPSCs) with the FTD-causing V337M *MAPT* mutation (tau^{V337M}) (Hong et al., 1998; Karch et al., 2019; Sohn et al., 2019; Spina et al., 2017) and WT isogenic controls (tau^{WT}). iPSCs

and their subsequent conversion to iNs by expression of neuronal transcription factors offer a clinically relevant model of human tau pathogenesis in a disease-specific genetic background (Ehrlich et al., 2015; Jiang et al., 2018; Nakamura et al., 2019; Silva et al., 2016; Sohn et al., 2019). Following up on our previous study using the neoepitope mAbs against caspase-cleaved tau at D13 and D402 sites in human AD and primary tauopathies (Theofilas et al., 2022), we evaluated tau proteolysis in the iNs and a human postmortem brain with the same V337M *MAPT* mutation. Our results demonstrate a time-dependent accumulation of caspase-cleaved tau and increased vulnerability to acute apoptotic stress in the tau^{V337M} iNs from 1 to 3 months post-differentiation that was reversed by inhibition of effector caspases, including caspase-6. This study offers insights into the potential of caspase-6 and other caspases as targets for therapeutic intervention against tau pathology in FTLD and other tauopathies.

Material and Methods

Development of caspase-6 cleaved tau neoepitope monoclonal antibodies

To address the absence of mAbs against tau sites primarily associated with caspase-6, we generated neoepitope mAbs against cleaved tau at D402 (mAbD402; 1-402) and D13 (mAbD13; 14-441) (Fig. 1-a), as previously described (Theofilas et al., 2022). Briefly, we produced the mAbs by immunizing 6-8-week-old wild-type Balb/c and SJL mice (SLAC) with keyhole limpet hemocyanin (KLH) conjugated tau peptides using protocols approved by ChemPartner IACUC committee. Blood samples from each mouse were collected one week after each immunization. The antibody titer and specificity were determined by enzyme-linked immunosorbent assay (ELISA) analysis and immunofluorescence (See Supplemental Experimental Procedures).

Mice with specific immune responses against tau peptides and proteins were selected for fusion and were given a final boost by intraperitoneal injection of 100 μg of the corresponding immunogen. After four days, mice were sacrificed and single-cell suspensions of splenocytes were prepared in NH_4OH at 1% (w/w), followed by centrifugation at 1000 rpm and washes with DMEM (Invitrogen). Viable splenocytes were fused with mouse myeloma cells SP2/0 (ATCC) at a ratio of 5:1 with high-efficiency electric fusion (BTX ECM200). 14 days after cell fusion, hybridoma supernatants were collected and screened by ELISA. The antibody isotypes were determined, and ELISA and western blot were used to test their ability to bind to tau. Clones that showed desired reactivity and specificity against tau were subjected to subcloning to produce stable monoclonal hybridoma cells. The reactivity and specificity of purified mAb.D13 and mAb.D402 were confirmed by ELISA against tau proteins and peptides (Fig. S1).

Human postmortem tissue processing and immunohistochemistry

Paraffin-embedded tissue sections cut at 8 μm from the temporal cortex of an individual with tau^{V337M} and manifested as behavioral variant frontotemporal dementia (68 years, female) were sourced from the Neurodegenerative Disease Brain Bank at the University of California, San Francisco. Immunohistochemistry was performed on de-paraffinized and rehydrated sections, following quenching of endogenous peroxidases with 3% H_2O_2

in methanol (Sigma) for 30 min and antigen retrieval in Tris-EDTA buffer/PBS with 0.05% Tween (Sigma) for 5 min at 121C in the autoclave. Sections were blocked in 5% milk/PBS with 0.05% Tween for 30 min and incubated with primary antibodies (TauC3 (D421), Invitrogen, AHB0061, mouse, 1:500; Active caspase-6 (cleaved at Asp179), Aviva Systems, OAAF05316, rabbit, 1:500; mAb.D402, ChemPartner, clone 47G7B5, mouse, 1:500; mAb.D13, ChemPartner, clone 5G4-1C5, mouse, 1:500) overnight at room temperature. After three washes with PBS-T (0.05% Tween-20), sections were incubated with the corresponding biotinylated secondary antibodies, followed by DAB or Red AP chromogen incubation based on manufacturer's instructions (Vector labs) and counterstained with hematoxylin (Sigma).

Cell lines

iPSC-derived induced neurons (iNs) with heterozygous V337M *MAPT* mutation (tau^{V337M}) and WT isogenic controls (tau^{WT}) were generated as previously described (Sohn et al., 2019; Wang et al., 2017). The Neurogenin 2 (Ngn2)-integrated iPSC line was created from a tau^{WT} human iPSC line (male; WTC11) (Miyaoka et al., 2014; Wang et al., 2017). The Tet-ON 3G-controlled Ngn2 transgene was integrated into the AAVS1 locus of human iPSC lines through a TALEN nuclease pair (Wang et al., 2017). CRISPR/Cas9 gene editing by homologous recombination was used to introduce the tau^{V337M} into the Ngn2-integrated iPSCs. Briefly, iPSCs were transfected with the Human Stem Cell Nucleofector Kit (Lonza) with sgRNA (5'-CTTGTGGGGTCA-TGGTTTACAGG-3' for V337M) plasmid (Addgene, 68463), Cas9 plasmid, and donor DNA plasmid containing a neomycin-resistance cassette (adapted from Addgene, PL552). Transfected cells were selected with neomycin for one week. Neomycin-resistant clones were selected and verified by genomic PCR and DNA sequencing. After sequence validation of the tau^{V337M} site, 1 mM Cre recombinase (Excellgen) was added to remove the neomycin-resistance cassette from gene-targeted iPSCs. Moreover, the top 10 potential off-target sites were sequenced and for each genotype, the correct clones were karyotyped (Cell Line Genetics) and expanded for subsequent experiments. iNs were differentiated using a two-step protocol (see Supplemental Experimental Procedures). For a detailed methodology on the generation of the iPSC lines, please refer to Sohn et al., 2019 and Wang et al., 2017.

Western blot protein analysis

Western blot analysis was performed using the Mini-PROTEAN Tetra system (Biorad) and standard immunoblotting techniques. See Supplemental Experimental Procedures for detailed methods.

Cell assays and compound treatment

iNs cultured in 96-well plates were treated with either vehicle (DMSO) or staurosporine (STS) and the pan-caspase inhibitor z-VAD-fmk (Enzo Lifesciences) directly in the media. Following 6h treatment, caspase-3/7 levels were examined using Caspase-Glo 3/7 (Promega) according to the manufacturer's instructions.

An ELISA based on lamin A cleavage, a specific substrate of active caspase-6, was used for detection and quantification of caspase-6 activity as previously described (Ehrnhoefer

et al., 2011). Briefly, iNs were treated with either vehicle (DMSO) or staurosporine (STS) and the caspase-6 inhibitor z-VEID-fmk (Enzo Lifesciences) directly in the media for 48h. Next, cells were fixed with 4% paraformaldehyde (Thermo Fisher Scientific) in PBS for 15 min and blocked with 5% bovine serum albumin (Sigma) in PBS with 0.01% Triton X-100 for 1h at room temperature. Cells were then incubated with cleaved lamin A primary antibody (Cell Signaling, 2035, rabbit, 1:200) overnight at 4°C, followed by an HRP-conjugated secondary antibody incubation (Invitrogen) for 1h at room temperature (GE Healthcare, NA934V, donkey anti-rabbit, 1:1000) a 5 min incubation with chemiluminescent HRP substrate (Thermo Fisher Scientific), and reading with a Spectramax microplate reader (Molecular Devices). iN cytotoxicity was measured using lactate dehydrogenase (LDH) release assay (Promega) following 48h treatment with vehicle (DMSO), STS, or STS/z-VAD-fmk according to the manufacturer's instructions. Readings were performed with a Spectramax microplate reader, followed by western blot or immunocytochemistry analysis.

To examine the morphological effects of STS and the z-VAD-fmk treatment in the iNs, we performed automated quantification of neurite length using IN Cell Developer Toolbox analysis routines based on image stacks uploaded from the IN Cell Analyzer 6500 confocal imager (GE Healthcare). To accommodate treatment-induced variation of neurite morphology during image acquisition, the Software Autofocus function was chosen to optimize the focal plane for each imaging field. DAPI was used for nuclei detection and microtubule-associated protein 2 (MAP2) for the detection of the cytoplasm and neurites. Mean neurite length per cell was calculated by subtracting a binary image of the cell body from a binary image of the entire cell, including the neurites. Data were obtained from 3-7 replicate wells per condition and an average of 1.5-2K cells per well. For IF analysis, fixed neurons were imaged using an IN Cell Analyzer 6500HS confocal imager (GE Healthcare). For further details see Supplemental Experimental Procedures.

Statistics

Statistical analyses and graphics were generated using R Statistical Software (version 3.6.1; R Foundation for Statistical Computing, Vienna, Austria). Groupwise differences were analyzed by comparing means (student's t-test, one or two-way ANOVA with post hoc Tukey tests) with the family-wise error rate set to 0.05 to correct for multiple comparisons. Data from at least three independent experiments are presented as mean ± SEM.

Results

Generation of caspase-6 cleaved tau neoepitope monoclonal antibodies

Besides TauC3 (D421), mAbs that recognize specific caspase-cleaved tau epitopes have been crucially missing. We recently developed two neoepitope mAbs against D13 and D402 tau cleavage sites (Fig. 1-a) using hybridoma technology. Neoepitope antibodies selectively bound to cleaved tau (1-402 or 14-441) but not full-length tau (1-441) as detected by ELISA (Fig. S1-a,b) and western blot analyses (Theofilas et al., 2022). Antibody specificity was also confirmed by immunofluorescence (IF) and antigen competition assays (Fig. S1-c) where mAb.D402 and mAb.D13 primary antibodies were preincubated with the cognate peptides used as immunogens (Table S1), resulting in loss of antibody signal. Together

with TauC3, mAb.D402, and mAb.D13 neoepitope antibodies were used to identify caspase-mediated pathological changes in postmortem brains and tau^{V337M} and tau^{WT} iNs.

Tau pathological changes in postmortem brains of FTLD and AD patients

To explore if D13 and D402 tau changes are present in the human postmortem brains with pathological tau accumulation we conducted a quantitative neuropathology study including cases of AD and other tauopathies such as progressive supranuclear palsy, corticobasal degeneration, and Pick's disease (Theofilas et al., 2022). D13 and D402 tau were more prominent in neurons of AD and Pick's disease cases. In both cases, most of the neurons positive for active caspase-6 also were positive for D13/D402. Here, we immunostained sections from the temporal cortex of an FTLD tau^{V337M} carrier using multiplex immunofluorescence methods targeting active caspase-6 and caspase-cleaved tau markers (Fig. 1-b). We detected positivity for TauC3 and mAb.D402 (red) in the cytoplasm and neurites that partially co-occurred with active caspase-6 but no positivity for mAb.D13. Taken together, our results show that neoepitope mAbs label pathological tau inclusions in FTLD-tau and corroborate the presence of active caspase-6 in the human brain seen in earlier studies (Theofilas et al., 2022, 2018).

Characterization of iPSC-induced neurons

Considering that tau^{V337M} causes FTD in humans, we generated heterozygous tau^{V337M} iNs and isogenic tau^{WT} controls to examine the disease mechanisms involving caspase activation and cleaved tau pathology in a clinically relevant cell culture model. Neuronal induction of a well-characterized human tau^{WT} line was performed using TALEN-based integration of a doxycycline-inducible *Ngn2* transgene into the AAVS1 safe harbor as previously described (Sohn et al., 2019; Wang et al., 2017). CRISPR/Cas9 genome editing was used to introduce the tau^{V337M} into tau^{WT} iPSCs to study the mutation's effects in isolation from the donor's genetic background. Both iPSC groups had a normal karyotype (Fig. S2-a) and typical colony-type morphology (Fig. 2-a). Moreover, genomic DNA sequencing of tau^{V337M} and tau^{WT} iPSCs confirmed the presence of the heterozygous tau^{V337M} in exon 12 (Fig. S2-b), and homogeneous expression of the pluripotency markers NANOG, OCT4, and SOX2 (Fig. S2-c) in the iNs confirmed the absence of NGN2 expression leakage without the addition of doxycycline. Following doxycycline treatment, iNs exhibited neuron-like morphology in 5-7 days and mature neuronal morphology between 3-4 weeks (Fig. 2-a).

One-month-old iNs were positive for the microtubule-associated protein 2 (MAP2) neuronal marker in the cytoplasm and neurites, and for the deep and upper cortical nuclear markers CTIP2 and SATB2, respectively, as confirmed by IF (Fig. 2-b). iNs were also positive for the glutamatergic marker vesicular glutamate transporter 1 (VGlut1) in the cytoplasm and neurites, an anticipated outcome of the *NGN2* expression (Sohn et al., 2019; Zhang et al., 2013). Overall, our findings demonstrate that at one-month post-differentiation, iNs exhibit neuron-specific morphology and express cortical and glutamatergic markers.

Increased levels of pathological tau in the tau^{V337M} neurons

Since FTLD-tau is characterized by progressive accumulation of toxic tau species and neuronal loss, we examined the presence and temporal course of tau pathological

accumulation of the tau^{V337M} in the mutant iNs relative to WT isogenic controls. We compared iNs cultured from 1 to 3 months post differentiation using western blot and a panel of tau antibodies, including total and oligomeric tau, 3R and 4R tau, and caspase-cleaved tau (Fig. 3).

Protein analysis using the total tau antibody HT7 showed positivity for distinct molecular weight bands corresponding to separate tau isoforms (Fig. 3-a). Tau antibody specificity was confirmed by the recombinant human tau ladder included here as an approximate guide of the tau isoform placement as it lacks the tau PTMs present in the cell lysates that could influence tau molecular weight. In agreement with previous studies showing enriched 3R tau levels in early neuronal development (Hefti et al., 2018; Iovino et al., 2015), we detected predominantly 3R isoform expression in the iNs and minimal 4R tau levels, both in tau^{V337M} and tau^{WT} iNs (Fig. 3-a). Antibody specificity for 3R and 4R tau was confirmed by the positivity of the respective isoform bands in the recombinant tau ladder. Total tau levels were comparable between the mutant and control iNs (Fig. S3-a), suggesting that any changes in the amount of pathological tau between the two groups were likely *MAPT* mutation-dependent and not due to changes in the overall tau levels.

Oligomeric tau aggregates could represent highly toxic and pathologically significant tau species in tauopathies (Puangmalai et al., 2020). We, therefore, investigated the presence and temporal changes of oligomeric and misfolded tau aggregates recognized by the antibody T18 (Lo Cascio et al., 2020) and non-denaturing conditions to preserve the original folded state of tau (Fig. 3-b). Standard loading controls are unsuitable for native Western blotting because proteins maintain their natural conformation, which hinders antibody binding to specific epitopes. To ensure loading reproducibility, we conducted three independent native Western blots that confirmed consistent effects for oligomeric (T18) and conformational (MC1) tau under non-denaturing conditions (see Supplemental Experimental Procedures, Fig. S3-b-d). To estimate the molecular weight of the native proteins, we used a protein standard for native electrophoresis stained with Coomassie Blue for band visualization. We detected elevated oligomeric tau levels in tau^{V337M} iNs relative to controls at 2 and 3 months post-differentiation. The protein standard revealed bands at 480–1,048 kD molecular weight, corresponding to tau oligomers, with no tau detected below that range. Conformational tau species identified by the MC1 antibody (Jicha et al., 1997) represent one of the most commonly detectable pathological features of tauopathies. Using the same experimental approach, we probed iN lysates using native electrophoresis. We observed a similar band pattern to T18, with elevated levels of conformational tau present after two months of culture only in the mutant iNs (Fig. 3-b, Fig. S3-b-d). Overall, our results indicated a time-dependent increase of tau toxic species in the form of oligomeric and conformationally modified tau in the mutant iNs compared to controls at two months post-differentiation, but not earlier. Next, we examined the temporal changes in phospho-tau and caspase-cleaved tau levels in the iNs using the anti-phospho-tau mAb PHF1 (Ser396/404), an epitope that is phosphorylated early in tau inclusion formation in humans (Mondragón-Rodríguez et al., 2014), and three caspase-cleaved tau mAbs, including cleavage sites primarily associated with activated caspase-6, D402 and D13, and the D421 site cleaved by multiple caspases (Gamblin et al., 2003; Rissman et al., 2004). Semi-quantitative analyses of GAPDH-normalized band intensities revealed a 2.5-fold increase of PHF-1 levels in

tau^{V337M} relative to controls at three months post-differentiation but not earlier (Fig. 3-c). Similarly, caspase-cleaved tau levels showed a 2.5 to 3-fold increase of D421 and D402-positive bands and a 2-fold increase of the D13 in tau^{V337M} iNs relative to controls at three months post differentiation. Again, these differences were absent in younger cells (Fig. 3-d-f). Altogether, our results demonstrate a significantly higher accumulation of phospho-tau and caspase-cleaved tau in tau^{V337M} iNs relative to controls that accumulated at three months post-differentiation, but not at earlier stages.

Caspase inhibition is neuroprotective against stress-induced cytotoxicity in the tau^{V337M} neurons

To test whether tau^{V337M} iNs are more vulnerable to stressors relative to controls, we treated three-month tau^{V337M} iNs with increasing concentrations of the wide-spectrum kinase inhibitor and apoptosis-inducer staurosporine (STS) for up to 48h. Treatment was followed by the detection of cytotoxicity levels measured by lactate dehydrogenase (LDH) release (Fig. S4). We observed a 2-fold increase in cytotoxicity levels in the tau^{V337M} iNs relative to tau^{WT} controls, using 40 μM STS for 48h (Fig. S4-b), and selected this condition for further studies. Cytotoxicity was significantly reduced by treatment with the pan-caspase inhibitor z-VAD-fmk (300 μM for 48h or 4 x 75 μM in 12h intervals; Fig. S4-c), indicating that cell death occurred via apoptosis.

Based on these established conditions (Fig. S4), we exposed iNs to 40 μM STS for 48h and increasing doses of z-VAD-fmk (300 and 600 μM; Fig. 4). Tau^{V337M} and tau^{WT} iNs treated with vehicle (DMSO) or z-VAD-fmk (600 μM) in the absence of STS showed low LDH release (Fig. 4); hence, baseline levels of apoptosis were low for iNs cultured for three months. Following STS treatment, however, we observed almost a 5-fold increase in cytotoxicity in the tau^{V337M} iNs compared to a 4-fold increase in control iNs. The mutant group was significantly more vulnerable to cytotoxicity following acute stress by STS ($p < 0.001$). Moreover, STS co-treatment with z-VAD-fmk significantly reversed cytotoxicity levels in the mutant iNs. Overall, our results demonstrated increased vulnerability to apoptotic cell death in tau^{V337M} iNs that was ameliorated by caspase inhibition.

To assess specific changes in the activity of caspase -6 and -3/7 between the tau^{V337M} and tau^{WT} iNs following stress exposure, we treated three-month tau^{V337M} and control iNs with STS and measured caspase activity. Caspase-6 activity was measured by ELISA for cleaved lamin A, a selective substrate of caspase-6 over other caspases (Mintzer et al., 2012), while Caspases-3/7 activity was measured using a DEVD-aminoluciferin substrate assay (Fig. 5). We observed a 4-fold increase in caspase-6 activity in the tau^{V337M} iNs compared to a 1-fold increase in control iNs following 20 μM STS treatment for 48h (Fig. 5-a), indicating that the mutant group had significantly higher caspase-6 activity relative to controls ($p < 0.01$). Notably, STS co-treatment with 10 μM of the caspase-6 inhibitor z-VEID-fmk significantly reversed caspase-6 activity levels in the mutant iNs ($p < 0.001$, z-VEID-FMK/STS vs STS alone). We also observed a 6-fold increase in active caspase-3/7 levels (Fig. 5-b) in the tau^{V337M} and tau^{WT} treated with 40 μM STS for 6h; there was no significant difference between caspase-3/7 activity between tau^{V337M} and tau^{WT} iNs. Caspase activity was reversed to baseline levels after the addition of 300 μM of the pan-caspase inhibitor

z-VAD-fmk. Overall, these results demonstrate that STS treatment induced apoptotic cell death and a marked increase in caspase activity in the iNs that were suppressed by caspase inhibition. Caspase-6, but not caspases-3/-7, was preferentially activated in the tau^{V337M} iNs relative to controls.

Next, we performed western blot analyses using lysates of iNs treated with 40 μM STS and 300 μM z-VAD-fmk (Fig. 5-c-d). Following STS treatment, we observed a statistically significant 2-fold increase in TauC3 binding in the tau^{V337M} iNs treated with STS compared to vehicle-treated cells ($p < 0.001$). TauC3 binding was not increased in control iNs treated with STS. In line with the cytotoxicity data (Fig. 4), STS co-treatment with z-VAD-fmk in tau^{V337M} iNs reversed TauC3 binding to baseline levels.

Stress-induced reduction of neurite length is rescued by caspase inhibition

The reduction in neurite length is a morphological indicator of compromised cell viability and neurotoxicity (Ehrlich et al., 2015; Wheeler et al., 2015). To examine the phenotypic effects of STS and z-VAD-fmk treatment on neurites in mutant and control iNs, we used immunocytochemistry (ICC) with DAPI to label cell nuclei (blue), and MAP2 (red) to label cytoplasm and neurites (Fig. 6a). Cells were imaged and subjected to automated quantification of neurite length after treatment with STS and z-VAD-fmk for the same duration and concentration and as our cytotoxicity assay (Fig. 4). We observed comparable mean neurite length in untreated iNs; neurite lengths were reduced upon treatment with 40 μM STS by 1.6-fold for tau^{V337M} ($p < 0.0001$) and 1.3-fold ($p< 0.0001$) for tau^{WT} (Fig. 6-b). Co-treatment of STS with z-VAD-fmk partially restored neurite length and preserved MAP2-positive processes in tau^{V337M} iNs compared to STS-treated cells ($p < 0.01$). For tau^{WT} iNs, neurite length in STS-treated cells was also restored upon the addition of z-VAD-fmk ($p < 0.05$). These data further demonstrate that neurotoxicity following STS treatment in the iNs was significantly caspase-dependent.

Discussion

Here, we induced glutamatergic iN with a pathological tau mutation and isogenic controls as models to investigate the build-up and role of caspase-6 truncated tau and the effects of inhibiting caspase activation in the pathological phenotype. We observed an age-dependent accumulation of pathogenic tau, including caspase-cleaved tau, phospho-tau, and oligomeric tau, in cells containing pathogenic tau^{V337M}. Three-month-old tau^{V337M} iNs post-differentiation showed a three-fold increase in caspase-cleaved D402 and D13 tau protein levels and increased phospho-tau and oligomeric tau species compared to isogenic controls. These mutant cells were also more sensitive to caspase-6 activation and apoptosis following acute treatment with STS, but treatment with caspase inhibitors rescued the phenotype. Altogether, these results demonstrate the significance of caspase activation and highlights the therapeutic potential of caspase inhibitors. The data are also consistent with the hypothesis that caspase-truncated tau is involved in the pathogenesis of tauopathies.

Active caspases are known to directly cleave tau, resulting in species that have a heightened tendency for self-aggregation and formation of cytoplasmic inclusions in neurons (Guillozet-Bongaarts et al., 2006; Guo et al., 2004; Horowitz et al., 2004; Rissman et al., 2004). In

particular, caspase-6 is a protease closely associated with NFT formation and neuronal loss in the human AD brain (Foveau et al., 2016; Guo et al., 2004; Ramcharitar et al., 2013; Theofilas et al., 2022, 2018). However, much of this existing evidence comes from animal models and immortalized cell lines, which might not accurately reflect the clinical phenotype. Our study innovates by using a synergistic approach combining a disease-relevant, iPSC-derived human neuronal model, novel mAbs for detecting caspase-6 cleaved tau species, and targeted pharmacological intervention against caspase activity to investigate the significance of active-caspase activation and caspase-truncated tau in the pathogenesis of tauopathies. This comprehensive strategy provides a more clinically relevant insight into the mechanisms driving tauopathies and the potential of caspase inhibition as a therapeutic approach.

Most studies restrict the duration of neuronal culture due to the technical challenges associated with sustaining neuronal lines over extended periods. However, the physiological increase of phospho-tau in developing neurons, a well-documented occurrence both *in vitro* and in human brains, complicates the interpretation of experimental outcomes conducted with neurons in developmental stages. In contrast, we cultured tau^{V337M} and tau^{WT} induced neurons (iNs) for at least three months post-differentiation. This approach was taken to circumvent the artefactual effects that arise from young age-related increases in phospho-tau expression observed in developing neurons. (Fiock et al., 2020; Hefti et al., 2018). Several of the differences detected between tau^{V337M} and tau^{WT} iNs only became apparent in iNs cultured for at least two to three months. Western blot protein analysis of 1–3-month cultured iNs revealed a time-dependent upregulation of T18 oligomeric tau and MC1 conformational tau at two months in the tau^{V337M} iNs relative to controls post-differentiation. Phospho-tau levels recognized by the PHF-1 antibody increased in the tau^{V337M} iNs relative to controls only at the three-month mark, underscoring the importance of utilizing more mature neurons in studies of tau pathology, despite needing more meticulous and costly technical protocols.

Transgenic mice expressing V337M human tau exhibited neurodegeneration and phospho-tau accumulation in the hippocampus, and behavioral abnormalities (Tanemura et al., 2002). In our previous study, we demonstrated that tau D402 and D13 are much more frequently found in tauopathies with 3-repeat tau such as AD and Pick's disease than those with a 4-repeat tau component only (Theofilas et al., 2022). *MAPT* V337M mutation inclusions in the human brain are positive for 3-repeat and 4-repeat tau (Karch et al., 2019). Finally, we detected D402 neuronal inclusions in the brain tissue of a subject who developed FTLD due to *MAPT* V337M mutation. Thus, we chose to derive iNs with tau^{V337M} *MAPT* mutation for our experiments on caspase-truncated tau because this is a well-characterized model featuring many similarities to human tauopathies, including time-dependent accumulation of pathological tau. These iNs also display increased vulnerability to stressors compared to isogenic controls (Silva et al., 2016), likely due to increased pathogenic tau levels and a lower capacity to survive additional stress (Ehrlich et al., 2015). Tau^{V337M} iNs also show tau cleavage at D421, tau detachment from microtubules, compromised axonal transport, and dysregulation of neuronal excitability (Ehrlich et al., 2015; Sohn et al., 2019). Thus, our results reproduced most of the findings reported by other studies using Tau^{V337M} iNs, which gave us confidence in this model for investigating the underexplored caspase-6 cleaved tau

D402 and D13, which we could do thanks to our novel mAb.D402 and mAb.D13 neoepitope antibodies.

Interestingly, while iN treatment with STS led to activation of caspase-3 and -7 was seen in both tau^{V337M} and tau^{WT}, high levels of caspase-6 were seen only in the tau^{V337M}. The selective upregulation of active caspase-6 suggests that increased cell death following acute stress in the tau^{V337M} iNs could be caspase-6 related. This aligns with prior research in human primary neurons, where caspase-6, but not caspase-3, was triggered by serum deprivation, leading to cell death upon the microinjection of recombinant active caspase-6 and -3. (LeBlanc et al., 1999; Zhang et al., 2000). Our results highlight and support previous suggestions of a central role of active caspase-6 in tauopathies.

It is important to acknowledge the limitations of our study. While our findings strongly indicate a notable role for caspase-6 compared to other effector caspases in tau truncation and neurotoxicity, we were unable to definitively identify which specific caspase(s) were responsible for tau cleavage in our cellular model because the peptidic z-VEID-fmk inhibitor is only partially selective for caspase-6 (Mintzer et al., 2012) and z-VAD-fmk caspase inhibitors are nonselective. Follow-up studies using highly selective, nonpeptidic inhibitors of caspase -6 that are currently under development are necessary to confirm our findings. Additionally, the use of one isogenic iPSC pair presents limitations, as a single genetic background may not capture the full spectrum of biological variability. Future studies will aim to replicate these findings in cells with diverse genetic backgrounds and *MAPT* mutations associated with tau pathology, ensuring a more comprehensive understanding of the disease mechanisms. Moreover, exploration of apoptosis-related substrates targeted by caspases -3 and -6 in addition to tau, including nuclear and mitochondrial proteins, could further clarify the mechanisms of caspase-mediated neurotoxicity in our cell model.

Conclusions:

In summary, our study demonstrates a time-dependent increase of tau cleavage and a pronounced vulnerability to stress and neuronal death in the tau^{V337M} iNs that is pharmacologically reversed by caspase inhibition. While both tau^{V337M} and tau^{WT} iNs respond to STS by activating caspases, tau^{V337M} iNs are more vulnerable to tau proteolysis and cell death after caspase activation. The collective evidence from our research and other studies underscores the critical role of caspase-6 and caspase-6 truncated tau in the development of tauopathies. This includes the observation that D13 and D402 tau neuronal inclusions are commonly found in Alzheimer's disease and appear to follow a pathway somewhat distinct from phospho-tau pathology. These findings highlight the need for more research focused on caspase-6 in tauopathies. They also suggest the potential of caspase-6 cleaved tau as a biomarker for Alzheimer's disease and point to caspase-6 inhibitors as promising therapeutic agents for combating tau-related neurodegenerative conditions.

Supplementary Material

Refer to Web version on PubMed Central for supplementary material.

Acknowledgments

We thank Wing Hung Lee, Mifrah Hayath, Grace Pohan, Steven Chen, and Daniel Medina-Cleghorn for technical support; Dr. Andrea LeBlanc for helpful discussions on caspase biochemistry; and Dr. Peter Davies for generously providing tau antibodies.

Funding

This study was supported by the National Institutes of Health K01AG053433 (P.T), K24AG053435, R56AG057528 and U54 NS100717 (L.T.G), P30AG062422 and P01AG019724 (B.L.M), R01AG054025 (R.K), UCSF RAP Pilot Award program (P.T), UCSF RAP Team Science Grant (L.T.G., M.R.A.), Alzheimer's Association AARG-16-441514 (L.T.G., M.R.A.), Rainwater Charitable Foundation (J.E.G; M.R.A.), and a Catalyst award from ShangPharma Innovation (M.R.A., T.Y., S.K, R.N.).

Abbreviations

AD	Alzheimer's disease
Asp	aspartic acid
ELISA	enzyme-linked immunosorbent assay
FTLD	frontotemporal lobar degeneration
HAT	hypoxanthine-aminopterin-thymidine
ICC	immunocytochemistry
IF	immunofluorescence
iNs	induced cortical neurons
iPSCs	induced pluripotent stem cells
KLH	keyhole limpet hemocyanin
LDH	lactate dehydrogenase
mAbs	monoclonal antibodies
MAP2	microtubule-associated protein 2
MAPT	Microtubule-associated protein tau
NFT	neurofibrillary tangle
Ngn2	Neurogenin 2
phospho-tau	tau hyperphosphorylation
PHFs	paired helical filaments
PTMs	post-translational modifications
STS	staurosporine
tau^{V337M}	V337M *MAPT* mutation

tau^{WT}	WT *MAPT*
VGlut1	vesicular glutamate transporter 1

References

Albrecht S, Bourdeau M, Bennett D, Mufson EJ, Bhattacharjee M, LeBlanc AC, 2007. Activation of caspase-6 in aging and mild cognitive impairment. Am. J. Pathol 170, 1200–1209. 10.2353/ajpath.2007.060974 [PubMed: 17392160]

Alonso AC, Grundke-Iqbal I, Iqbal K, 1996. Alzheimer's disease hyperphosphorylated tau sequesters normal tau into tangles of filaments and disassembles microtubules. Nat. Med 2, 783–787. 10.1038/nm0796-783 [PubMed: 8673924]

Angel A, Volkman R, Royal TG, Offen D, 2020. Caspase-6 Knockout in the 5xFAD Model of Alzheimer's Disease Reveals Favorable Outcome on Memory and Neurological Hallmarks. Int. J. Mol. Sci 21. 10.3390/ijms21031144

Cotman CW, Poon WW, Rissman RA, Blurton-Jones M, 2005. The role of caspase cleavage of tau in Alzheimer's disease neuropathology. J. Neuropathol. Exp. Neurol 64, 104–112. 10.1093/jnen/64.2.104 [PubMed: 15751224]

Cusack CL, Swahari V, Hampton Henley W, Michael Ramsey J, Deshmukh M, 2013. Distinct pathways mediate axon degeneration during apoptosis and axon-specific pruning. Nat. Commun 4, 1876. 10.1038/ncomms2910 [PubMed: 23695670]

de Calignon A, Fox LM, Pitstick R, Carlson GA, Bacskai BJ, Spires-Jones TL, Hyman BT, 2010. Caspase activation precedes and leads to tangles. Nature 464, 1201–1204. 10.1038/nature08890 [PubMed: 20357768]

Ehrlich M, Hallmann A-L, Reinhardt P, Araúzo-Bravo MJ, Korr S, Röpke A, Psathaki OE, Ehling P, Meuth SG, Oblak AL, Murrell JR, Ghetti B, Zaehres H, Schöler HR, Sterneckert J, Kuhlmann T, Hargus G, 2015. Distinct neurodegenerative changes in an induced pluripotent stem cell model of frontotemporal dementia linked to mutant TAU protein. Stem Cell Rep. 5, 83–96. 10.1016/j.stemcr.2015.06.001

Ehrnhoefer DE, Skotte NH, Savill J, Nguyen YTN, Ladha S, Cao L-P, Dullaghan E, Hayden MR, 2011. A Quantitative Method for the Specific Assessment of Caspase-6 Activity in Cell Culture. PLOS ONE 6, e27680. 10.1371/journal.pone.0027680 [PubMed: 22140457]

Enari M, Sakahira H, Yokoyama H, Okawa K, Iwamatsu A, Nagata S, 1998. A caspase-activated DNase that degrades DNA during apoptosis, and its inhibitor ICAD. Nature 391, 43–50. 10.1038/34112 [PubMed: 9422506]

Fiock KL, Smalley ME, Crary JF, Pasca AM, Hefti MM, 2020. Increased Tau Expression Correlates with Neuronal Maturation in the Developing Human Cerebral Cortex. eNeuro 7. 10.1523/ENEURO.0058-20.2020

Foveau B, Albrecht S, Bennett DA, Correa JA, LeBlanc AC, 2016. Increased Caspase-6 activity in the human anterior olfactory nuclei of the olfactory bulb is associated with cognitive impairment. Acta Neuropathol. Commun 4, 127. 10.1186/s40478-016-0400-x [PubMed: 27931265]

Gamblin TC, Chen F, Zambrano A, Abraha A, Lagalwar S, Guillozet AL, Lu M, Fu Y, Garcia-Sierra F, LaPointe N, Miller R, Berry RW, Binder LI, Cryns VL, 2003. Caspase cleavage of tau: linking amyloid and neurofibrillary tangles in Alzheimer's disease. Proc. Natl. Acad. Sci. U. S. A 100, 10032–10037. 10.1073/pnas.1630428100 [PubMed: 12888622]

Girling KD, Demers M-J, Laine J, Zhang S, Wang YT, Graham RK, 2018. Activation of caspase-6 and cleavage of caspase-6 substrates is an early event in NMDA receptor-mediated excitotoxicity. J. Neurosci. Res 96, 391–406. 10.1002/jnr.24153 [PubMed: 29193273]

Graham RK, Deng Y, Slow EJ, Haigh B, Bissada N, Lu G, Pearson J, Shehadeh J, Bertram L, Murphy Z, Warby SC, Doty CN, Roy S, Wellington CL, Leavitt BR, Raymond LA, Nicholson DW, Hayden MR, 2006. Cleavage at the caspase-6 site is required for neuronal dysfunction and degeneration due to mutant huntingtin. Cell 125, 1179–1191. 10.1016/j.cell.2006.04.026 [PubMed: 16777606]

Guillozet-Bongaarts AL, Cahill ME, Cryns VL, Reynolds MR, Berry RW, Binder LI, 2006. Pseudophosphorylation of tau at serine 422 inhibits caspase cleavage: in vitro evidence

and implications for tangle formation in vivo. J. Neurochem 97, 1005–1014. 10.1111/j.1471-4159.2006.03784.x [PubMed: 16606369]

Guo H, Albrecht S, Bourdeau M, Petzke T, Bergeron C, LeBlanc AC, 2004. Active caspase-6 and caspase-6-cleaved tau in neuropil threads, neuritic plaques, and neurofibrillary tangles of Alzheimer's disease. Am. J. Pathol 165, 523–531. 10.1016/S0002-9440(10)63317-2 [PubMed: 15277226]

Hefti MM, Farrell K, Kim S, Bowles KR, Fowkes ME, Raj T, Crary JF, 2018. High-resolution temporal and regional mapping of MAPT expression and splicing in human brain development. PLOS ONE 13, e0195771. 10.1371/journal.pone.0195771 [PubMed: 29634760]

Hong M, Zhukareva V, Vogelsberg-Ragaglia V, Wszolek Z, Reed L, Miller BI, Geschwind DH, Bird TD, McKeel D, Goate A, Morris JC, Wilhelmsen KC, Schellenberg GD, Trojanowski JQ, Lee VM, 1998. Mutation-specific functional impairments in distinct tau isoforms of hereditary FTDP-17. Science 282, 1914–1917. 10.1126/science.282.5395.1914 [PubMed: 9836646]

Horowitz PM, Patterson KR, Guillozet-Bongaarts AL, Reynolds MR, Carroll CA, Weintraub ST, Bennett DA, Cryns VL, Berry RW, Binder LI, 2004. Early N-terminal changes and caspase-6 cleavage of tau in Alzheimer's disease. J. Neurosci. Off. J. Soc. Neurosci 24, 7895–7902. 10.1523/JNEUROSCI.1988-04.2004

Iovino M, Agathou S, González-Rueda A, Del Castillo Velasco-Herrera M, Borroni B, Alberici A, Lynch T, O'Dowd S, Geti I, Gaffney D, Vallier L, Paulsen O, Káradóttir RT, Spillantini MG, 2015. Early maturation and distinct tau pathology in induced pluripotent stem cell-derived neurons from patients with MAPT mutations. Brain J. Neurol 138, 3345–3359. 10.1093/brain/awv222

Iqbal K, Grundke-Iqbal I, Zaidi T, Merz PA, Wen GY, Shaikh SS, Wisniewski HM, Alafuzoff I, Winblad B, 1986. Defective brain microtubule assembly in Alzheimer's disease. Lancet Lond. Engl 2, 421–426. 10.1016/s0140-6736(86)92134-3

Jiang S, Wen N, Li Z, Dube U, Del Aguila J, Budde J, Martinez R, Hsu S, Fernandez MV, Cairns NJ, Dominantly Inherited Alzheimer Network (DIAN), International FTD-Genomics Consortium (IFGC), Harari O, Cruchaga C, Karch CM, 2018. Integrative system biology analyses of CRISPR-edited iPSC-derived neurons and human brains reveal deficiencies of presynaptic signaling in FTLD and PSP. Transl. Psychiatry 8, 265. 10.1038/s41398-018-0319-z [PubMed: 30546007]

Jicha GA, Bowser R, Kazam IG, Davies P, 1997. Alz-50 and MC-1, a new monoclonal antibody raised to paired helical filaments, recognize conformational epitopes on recombinant tau. J. Neurosci. Res 48, 128–132. 10.1002/(SICI)1097-4547(19970415)48:2<128::AID-JNR5>3.0.CO;2-E [PubMed: 9130141]

Karch CM, Kao AW, Karydas A, Onanuga K, Martinez R, Argouarch A, Wang C, Huang C, Sohn PD, Bowles KR, Spina S, Silva MC, Marsh JA, Hsu S, Pugh DA, Ghoshal N, Norton J, Huang Y, Lee SE, Seeley WW, Theofilas P, Grinberg LT, Moreno F, McIlroy K, Boeve BF, Cairns NJ, Crary JF, Haggarty SJ, Ichida JK, Kosik KS, Miller BL, Gan L, Goate AM, Temple S, 2019. A Comprehensive Resource for Induced Pluripotent Stem Cells from Patients with Primary Tauopathies. Stem Cell Rep. 13, 939–955. 10.1016/j.stemcr.2019.09.006

Kim Y, Choi H, Lee W, Park H, Kam T-I, Hong S, Nah J, Jung S, Shin B, Lee H, Choi T-Y, Choo H, Kim K-K, Choi S-Y, Kayed R, Jung Y-K, 2016. Caspase-cleaved tau exhibits rapid memory impairment associated with tau oligomers in a transgenic mouse model. Neurobiol. Dis 87, 19–28. 10.1016/j.nbd.2015.12.006 [PubMed: 26704708]

Klaiman G, Petzke TL, Hammond J, Leblanc AC, 2008. Targets of caspase-6 activity in human neurons and Alzheimer disease. Mol. Cell. Proteomics 7, 1541–1555. 10.1074/mcp.M800007-MCP200 [PubMed: 18487604]

Ladha S, Qiu X, Casal L, Caron NS, Ehrnhoefer DE, Hayden MR, 2018. Constitutive ablation of caspase-6 reduces the inflammatory response and behavioural changes caused by peripheral pro-inflammatory stimuli. Cell Death Discov. 4, 1–10. 10.1038/s41420-018-0043-8

Lakhani SA, Masud A, Kuida K, Porter GA, Booth CJ, Mehal WZ, Inayat I, Flavell RA, 2006. Caspases 3 and 7: Key Mediators of Mitochondrial Events of Apoptosis. Science 311, 847–851. 10.1126/science.1115035 [PubMed: 16469926]

Lanata SC, Miller BL, 2016. The behavioural variant frontotemporal dementia (bvFTD) syndrome in psychiatry. J. Neurol. Neurosurg. Psychiatry 87, 501–511. 10.1136/jnnp-2015-310697 [PubMed: 26216940]

LeBlanc A, Liu H, Goodyer C, Bergeron C, Hammond J, 1999. Caspase-6 role in apoptosis of human neurons, amyloidogenesis, and Alzheimer's disease. J. Biol. Chem 274, 23426–23436. [PubMed: 10438520]

Lo Cascio F, Garcia S, Montalbano M, Puangmalai N, McAllen S, Pace A, Palumbo Piccionello A, Kayed R, 2020. Modulating disease-relevant tau oligomeric strains by small molecules. J. Biol. Chem 295, 14807–14825. 10.1074/jbc.RA120.014630 [PubMed: 32737202]

Mintzer R, Ramaswamy S, Shah K, Hannoush RN, Pozniak CD, Cohen F, Zhao X, Plise E, Lewcock JW, Heise CE, 2012. A whole cell assay to measure caspase-6 activity by detecting cleavage of lamin A/C. Plos One 7, e30376. 10.1371/journal.pone.0030376 [PubMed: 22253931]

Miyaoka Y, Chan AH, Judge LM, Yoo J, Huang M, Nguyen TD, Lizarraga PP, So P-L, Conklin BR, 2014. Isolation of single-base genome-edited human iPS cells without antibiotic selection. Nat. Methods 11, 291–293. 10.1038/nmeth.2840 [PubMed: 24509632]

Mondragón-Rodríguez S, Perry G, Luna-Muñoz J, Acevedo-Aquino MC, Williams S, 2014. Phosphorylation of tau protein at sites Ser(396-404) is one of the earliest events in Alzheimer's disease and Down syndrome. Neuropathol. Appl. Neurobiol 40, 121–135. 10.1111/nan.12084 [PubMed: 24033439]

Nakamura M, Shiozawa S, Tsuboi D, Amano M, Watanabe H, Maeda S, Kimura T, Yoshimatsu S, Kisa F, Karch CM, Miyasaka T, Takashima A, Sahara N, Hisanaga S-I, Ikeuchi T, Kaibuchi K, Okano H, 2019. Pathological Progression Induced by the Frontotemporal Dementia-Associated R406W Tau Mutation in Patient-Derived iPSCs. Stem Cell Rep. 10.1016/j.stemcr.2019.08.011

Nicholls SB, DeVos SL, Commins C, Nobuhara C, Bennett RE, Corjuc DL, Maury E, Eftekharzadeh B, Akingbade O, Fan Z, Roe AD, Takeda S, Wegmann S, Hyman BT, 2017. Characterization of TauC3 antibody and demonstration of its potential to block tau propagation. PLOS ONE 12, e0177914. 10.1371/journal.pone.0177914 [PubMed: 28531180]

Nikolaev A, McLaughlin T, O'Leary DDM, Tessier-Lavigne M, 2009. APP binds DR6 to trigger axon pruning and neuron death via distinct caspases. Nature 457, 981–989. 10.1038/nature07767 [PubMed: 19225519]

Novak M, Kabat J, Wischik CM, 1993. Molecular characterization of the minimal protease resistant tau unit of the Alzheimer's disease paired helical filament. EMBO J. 12, 365–370. 10.1002/j.1460-2075.1993.tb05665.x [PubMed: 7679073]

Puangmalai N, Bhatt N, Montalbano M, Sengupta U, Gaikwad S, Ventura F, McAllen S, Ellsworth A, Garcia S, Kayed R, 2020. Internalization mechanisms of brain-derived tau oligomers from patients with Alzheimer's disease, progressive supranuclear palsy and dementia with Lewy bodies. Cell Death Dis. 11, 314. 10.1038/s41419-020-2503-3 [PubMed: 32366836]

Ramcharitar J, Albrecht S, Afonso VM, Kaushal V, Bennett DA, Leblanc AC, 2013. Cerebrospinal fluid tau cleaved by caspase-6 reflects brain levels and cognition in aging and Alzheimer disease. J. Neuropathol. Exp. Neurol 72, 824–832. 10.1097/NEN.0b013e3182a0a39f [PubMed: 23965742]

Rissman RA, Poon WW, Blurton-Jones M, Oddo S, Torp R, Vitek MP, LaFerla FM, Rohn TT, Cotman CW, 2004. Caspase-cleavage of tau is an early event in Alzheimer disease tangle pathology. J. Clin. Invest 114, 121–130. 10.1172/JCI20640 [PubMed: 15232619]

Silva MC, Cheng C, Mair W, Almeida S, Fong H, Biswas MHU, Zhang Z, Huang Y, Temple S, Coppola G, Geschwind DH, Karydas A, Miller BL, Kosik KS, Gao F-B, Steen JA, Haggarty SJ, 2016. Human iPSC-Derived Neuronal Model of Tau-A152T Frontotemporal Dementia Reveals Tau-Mediated Mechanisms of Neuronal Vulnerability. Stem Cell Rep. 7, 325–340. 10.1016/j.stemcr.2016.08.001

Sohn PD, Huang CT-L, Yan R, Fan L, Tracy TE, Camargo CM, Montgomery KM, Arhar T, Mok S-A, Freilich R, Baik J, He M, Gong S, Roberson ED, Karch CM, Gestwicki JE, Xu K, Kosik KS, Gan L, 2019. Pathogenic tau impairs axon initial segment plasticity and excitability homeostasis. Neuron 104, 458–470.e5. 10.1016/j.neuron.2019.08.008 [PubMed: 31542321]

Spillantini MG, Goedert M, 2013. Tau pathology and neurodegeneration. Lancet Neurol. 12, 609–622. 10.1016/S1474-4422(13)70090-5 [PubMed: 23684085]

Spina S, Schonhaut DR, Boeve BF, Seeley WW, Ossenkoppele R, O'Neil JP, Lazaris A, Rosen HJ, Boxer AL, Perry DC, Miller BL, Dickson DW, Parisi JE, Jagust WJ, Murray ME, Rabinovici GD, 2017. Frontotemporal dementia with the V337M MAPT mutation: Tau-PET and pathology correlations. Neurology 88, 758–766. 10.1212/WNL.0000000000003636 [PubMed: 28130473]

Tanemura K, Murayama M, Akagi T, Hashikawa T, Tominaga T, Ichikawa M, Yamaguchi H, Takashima A, 2002. Neurodegeneration with Tau Accumulation in a Transgenic Mouse Expressing V337M Human Tau. J. Neurosci 22, 133–141. 10.1523/JNEUROSCI.22-01-00133.2002 [PubMed: 11756496]

Theofilas P, Ehrenberg AJ, Nguy A, Thackrey JM, Dunlop S, Mejia MB, Alho AT, Paraizo Leite RE, Rodriguez RD, Suemoto CK, Nascimento CF, Chin M, Medina-Cleghorn D, Cuervo AM, Arkin M, Seeley WW, Miller BL, Nitrini R, Pasqualucci CA, Filho WJ, Rueb U, Neuhaus J, Heinsen H, Grinberg LT, 2018. Probing the correlation of neuronal loss, neurofibrillary tangles, and cell death markers across the Alzheimer's disease Braak stages: a quantitative study in humans. Neurobiol. Aging 61, 1–12. 10.1016/j.neurobiolaging.2017.09.007 [PubMed: 29031088]

Theofilas P, Piergies AMH, Oh I, Lee YB, Li SH, Pereira FL, Petersen C, Ehrenberg AJ, Eser RA, Ambrose AJ, Chin B, Yang T, Khan S, Ng R, Spina S, Seeley WW, Miller BL, Arkin MR, Grinberg LT, 2022. Caspase-6-cleaved tau is relevant in Alzheimer's disease and marginal in four-repeat tauopathies: Diagnostic and therapeutic implications. Neuropathol. Appl. Neurobiol 48, e12819. 10.1111/nan.12819 [PubMed: 35508761]

Thornberry NA, Lazebnik Y, 1998. Caspases: enemies within. Science 281, 1312–1316. 10.1126/science.281.5381.1312 [PubMed: 9721091]

Wang C, Ward ME, Chen R, Liu K, Tracy TE, Chen X, Xie M, Sohn PD, Ludwig C, Meyer-Franke A, Karch CM, Ding S, Gan L, 2017. Scalable Production of iPSC-Derived Human Neurons to Identify Tau-Lowering Compounds by High-Content Screening. Stem Cell Rep. 9, 1221–1233. 10.1016/j.stemcr.2017.08.019

Wheeler HE, Wing C, Delaney SM, Komatsu M, Dolan ME, 2015. Modeling Chemotherapeutic Neurotoxicity with Human Induced Pluripotent Stem Cell-Derived Neuronal Cells. PLOS ONE 10, e0118020. 10.1371/journal.pone.0118020 [PubMed: 25689802]

Zhang Q, Zhang X, Sun A, 2009. Truncated tau at D421 is associated with neurodegeneration and tangle formation in the brain of Alzheimer transgenic models. Acta Neuropathol. (Berl.) 117, 687–697. 10.1007/s00401-009-0491-6 [PubMed: 19190923]

Zhang Y, Goodyer C, LeBlanc A, 2000. Selective and protracted apoptosis in human primary neurons microinjected with active caspase-3, -6, -7, and -8. J. Neurosci. Off. J. Soc. Neurosci 20, 8384–8389.

Zhang Y, Pak C, Han Y, Ahlenius H, Zhang Z, Chanda S, Marro S, Patzke C, Acuna C, Covy J, Xu W, Yang N, Danko T, Chen L, Wernig M, Südhof TC, 2013. Rapid single-step induction of functional neurons from human pluripotent stem cells. Neuron 78, 785–798. 10.1016/j.neuron.2013.05.029 [PubMed: 23764284]

Zhao Y, Tseng I-C, Heyser CJ, Rockenstein E, Mante M, Adame A, Zheng Q, Huang T, Wang X, Arslan PE, Chakrabarty P, Wu C, Bu G, Mobley WC, Zhang Y-W, St George-Hyslop P, Masliah E, Fraser P, Xu H, 2015. Appoptosin-Mediated Caspase Cleavage of Tau Contributes to Progressive Supranuclear Palsy Pathogenesis. Neuron 87, 963–975. 10.1016/j.neuron.2015.08.020 [PubMed: 26335643]

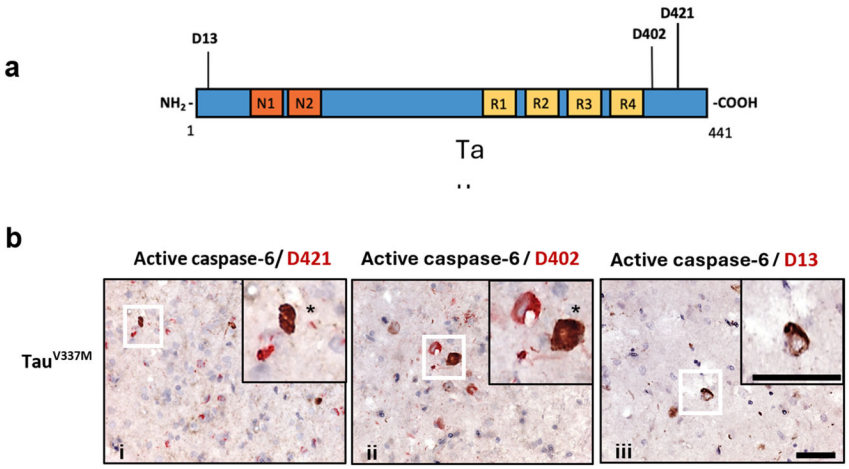

Figure 1.

Caspase-6 cleaved tau neoepitope antibody positivity in human postmortem brains with tau accumulation. (a) Schematic depicting two caspase-6 cleaved tau sites targeted by monoclonal neoepitope antibodies mAb.D13 (D13; 14-441) and mAb.D402 (D402; 1-402), at the N- and C-terminus of tau, respectively. The C-terminus D421 site of tau is targeted by the antibody TauC3 and cleaved by multiple caspases; (b) Brain sections from the temporal cortex of an individual with tau^{V337M} and FTD, showing antibody positivity for active caspase-6 (brown) and caspase-cleaved tau (red), including TauC3 (D421) (i), mAb.D402 (ii), and mAb.D13 (iii). Asterisks indicate cells positive for both active caspase-6 and caspase-cleaved tau markers. Scale bars: 50 μm.

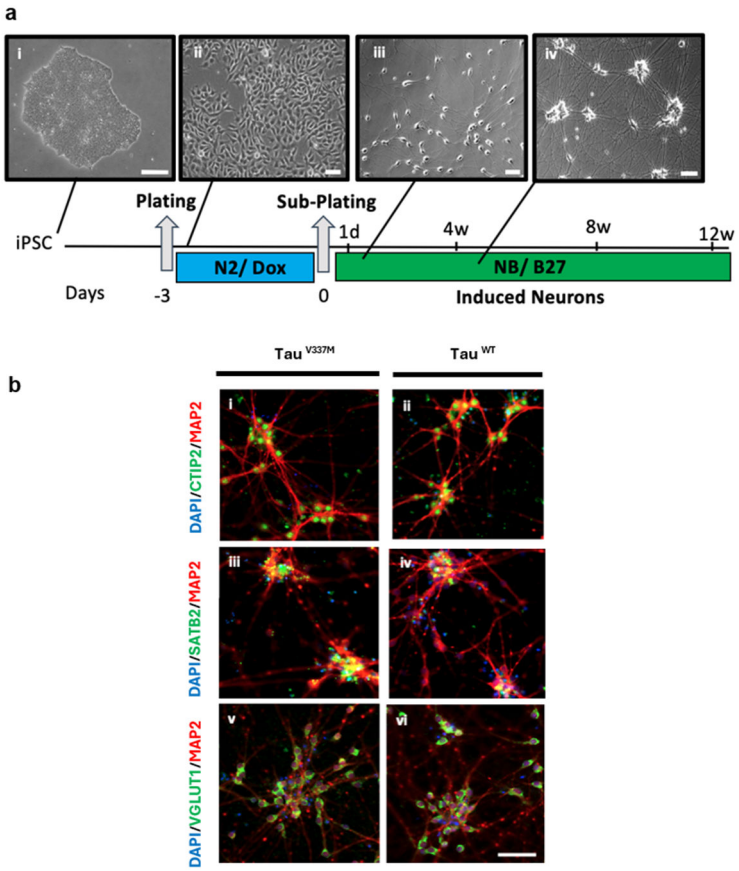

Figure 2.

Timeline of iPSC differentiation to neurons following doxycycline-inducible expression of Ngn2. (a) Phase-contrast images represent individual stages of the differentiation protocol, including iPSCs (i), neuronal precursors (ii), immature neurons (iii), and mature neurons (iv); (b) IF characterization of neurons at 1-month post differentiation. Mutant (tau^{V337M}) and control (tau^{WT}) neurons were positive for cortical (green; i-iv), glutamatergic (green; v-vi), and neuronal (red; i-vi) markers. Nuclei were stained with DAPI (blue; i-vi). Scale bars: (a) i: 200 μm, ii-iv: 50 μm (b) 60 μm.

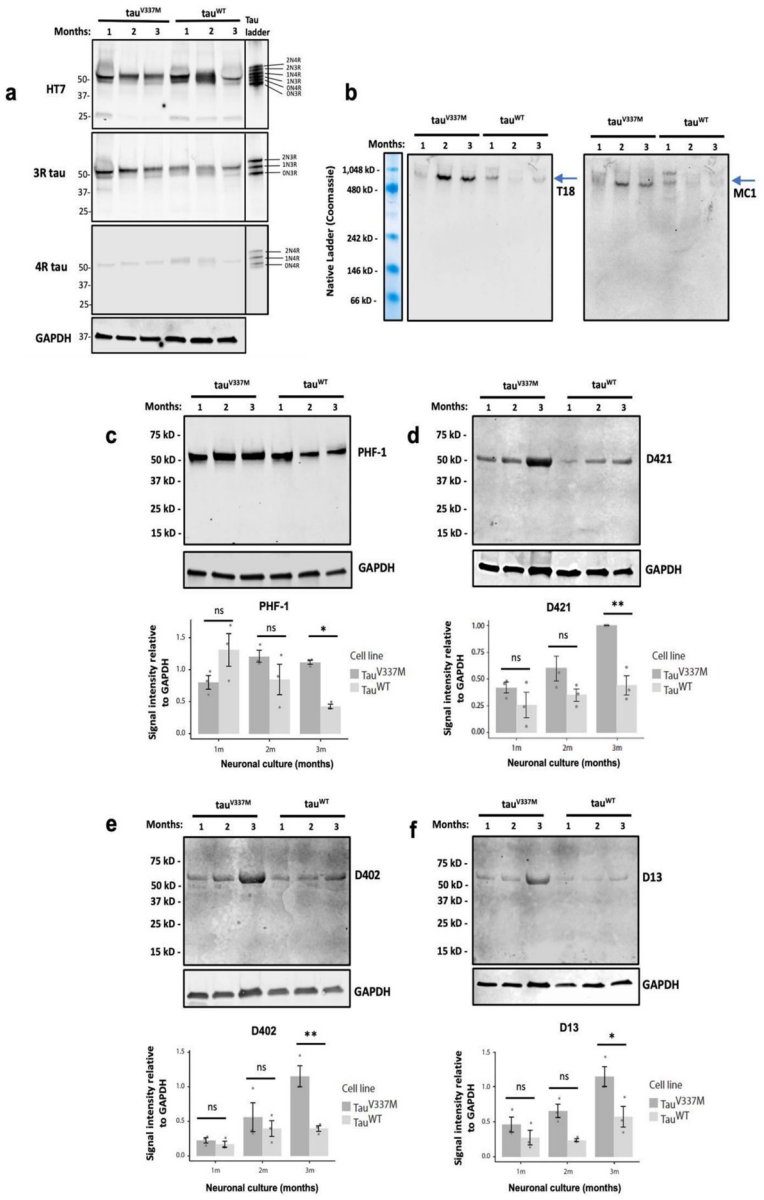

Figure 3.

Time-dependent tau pathological changes in the tau^{V337M} neurons detected by western blot analyses. (a) Expression of total tau (HT7) and tau isoforms (3R and 4R tau) in tau^{V337M} and tau^{WT} neurons cultured from 1 to 3 months. Antibody specificity was confirmed by a recombinant tau ladder containing all six tau isoforms (right panels); (b) Oligomeric (T18) and conformational (MC1) tau levels were detected under non-denaturing conditions for preserving protein conformation. The molecular weight of the proteins was estimated using a protein standard for native electrophoresis stained with Coomassie blue (far-left panel) for band visualization (see also Fig. S4); (c-f) Semi-quantification of p-tau (PHF-1) and caspase- cleave tau (D421, D402, and D13) protein levels based on band intensities relative to GAPDH internal loading control ($n \geq 3$ independent experiments; two-way ANOVA with post hoc Tukey test; ns, not significant: $p > 0.05$; *$p < 0.05$, **$p < 0.01$).

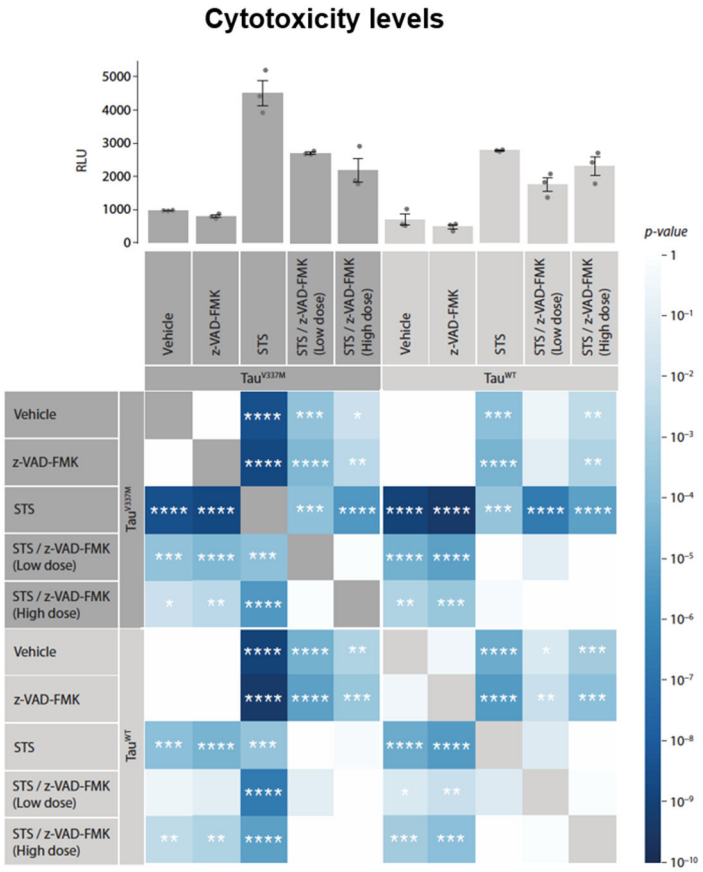

Figure 4.

Caspase inhibition is neuroprotective against acute stress-induced cytotoxicity in the tau^{V337M} neurons. Changes in cytotoxicity levels were measured by LDH release following a 48-hour treatment with STS and the pan-caspase inhibitor (z-VAD-fmk) in 3-month cultured neurons. The matrix heatmap illustrates p-values (color gradient) and significance levels (asterisks) between treatment groups. Dark gray shade represents tau^{V337M} and light gray shade represents tau^{WT} neurons (n=3 independent experiments; two-way ANOVA with post hoc Tukey test; *p < 0.05, **p<0.01, ***p<0.001, ****p<0.0001). RLU: Relative light units.

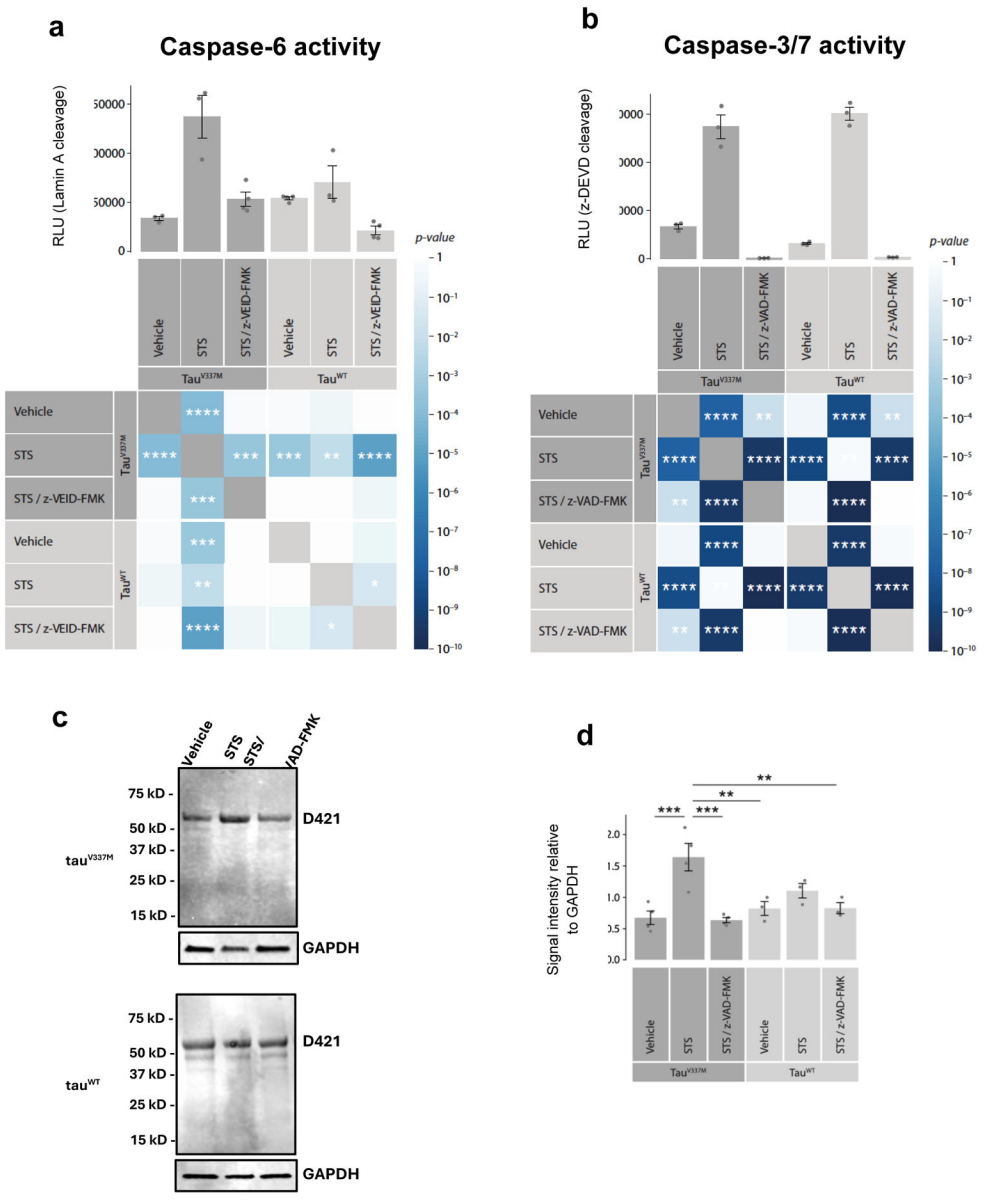

Figure 5.

Stress-induced caspase activation in the induced neurons. Active caspase-6 (a) and caspase-3/7 levels (b) were examined in 3-month cultured neurons using caspase-specific cleavage substrates following treatment with vehicle, STS, and STS/z-VEID-fmk (a caspase-6 inhibitor) or STS/z-VAD-fmk (a pan-caspase inhibitor). The matrix heatmap illustrates p-values (color gradient) and significance levels (asterisks) between treatment groups. Dark gray shade represents tau^{V337M} and light gray shade represents tau^{WT} neurons; (c-d) Semi-quantification of caspase-cleaved tau (D421) protein levels in neurons treated with STS or STS/z-VAD- fmk for 48h based on band intensities relative to GAPDH internal loading control (n ≥ 3 independent experiments; two-way ANOVA with post hoc Tukey test; *p < 0.05, **p<0.01, ***p<0.001, ****p<0.0001). RLU: Relative light units.

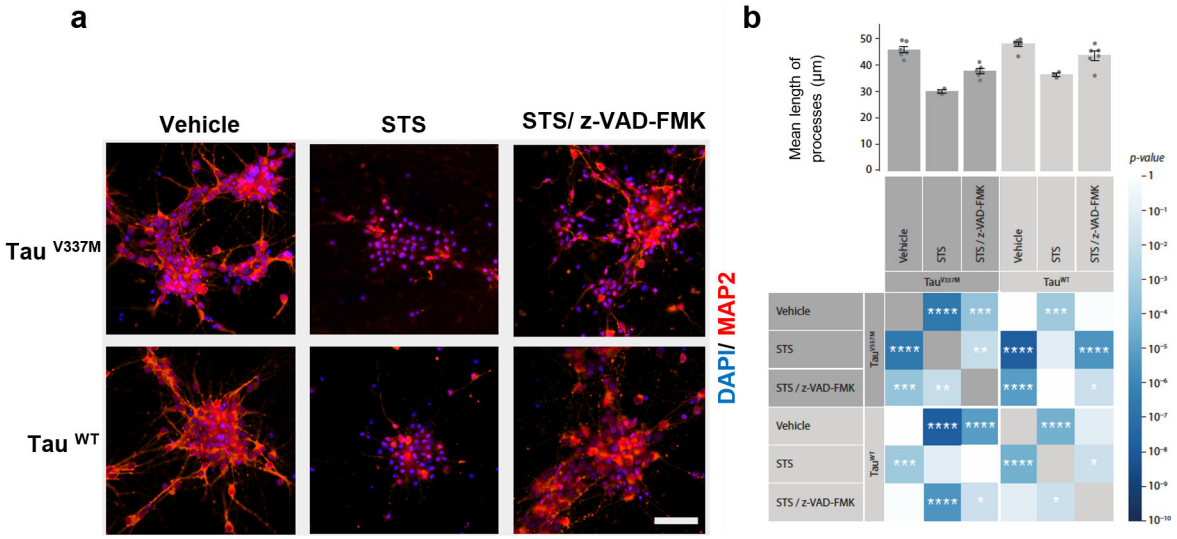

Figure 6.

Caspase inhibition rescues stress-induced reduction of neurite length in the induced neurons. (a) IF staining of neurites (MAP2, red) and cell nuclei (DAPI, blue) following a 48h treatment with STS and caspase-inhibitor (z-VAD-fmk) in 3-month cultured neurons; (b) Image quantification of mean length of processes (based on a). Matrix heatmap illustrates p-values (color gradient) and significance levels (asterisks) between treatment groups. Dark gray shade represents tau^{V337M} and light gray shade represents tau^{WT} neurons ($n \geq 3$ independent experiments; two-way ANOVA with post hoc Tukey test; *$p < 0.05$, **$p<0.01$, ***$p<0.001$, ****$p<0.0001$). Scale bar: 50 μm.